Effect of Frequency on Insulin Response to Electric Field Stress

Akin Budi,[†] F. Sue Legge,[†] Herbert Treutlein,[‡] and Irene Yarovsky*[,†]

Applied Physics, School of Applied Sciences, RMIT University, GPO Box 2476V, Melbourne, Victoria 3001, Australia, and Cytopia Research Pty. Ltd., PO Box 6492, St. Kilda Road Central, Melbourne, Victoria 8008, Australia

Received: November 3, 2006; In Final Form: March 2, 2007

There are many unanswered questions regarding the precise way in which proteins respond to external stress. Since the function of proteins is critically linked to their three-dimensional structures, exposure to any form of stress which may induce changes in conformation can potentially initiate severe cellular dysfunction. This is particularly relevant with regard to the increasing presence of electromagnetic devices in today's environment and the possible effects on human health. Previously, we investigated the effect of electric field of various strengths on insulin chain-B under static and oscillating conditions. This paper expands on our previous work by subjecting the peptide to an oscillating electric field of different frequencies. We observed a frequency-dependent effect where the application of lower-frequency oscillating fields resulted in static-field-like behavior of the peptide, whereby the intrinsic flexibility of the protein is constrained, thus potentially restricting access to the protein's active state.

1. Introduction

Over the last three decades, there have been advances in digital technology, such as microwaves and mobile communication devices, which are now a major part of our every day life. The constant increase in the development of this technology makes it extremely difficult to assess potential health effects of the steady exposure to electromagnetic radiation. The impact of electric and magnetic radiation exposure on human health is not well understood. Recent studies have shown evidence of a "non-thermal" effect from such devices which may cause changes in protein conformations.[1,2] However, the "non-thermal" effect may result from rapid temperature changes which are not detected by normal thermometry.[3] Yet, the rapid increase (few nanoseconds) in temperature can alter protein conformation, which in turn can change protein activity, causing harmful effects.

We have used molecular dynamics (MD) in our earlier work to reproduce the normal behavior of insulin chain-B under ambient conditions[4] and to predict the effects of stress, such as thermal and electric field, on the peptide.[4,5] In our previous study, we highlighted the difference in the mechanisms of the damage inflicted by the application of static and oscillating electric fields on the conformation of insulin chain-B.[5] The application of static field affects the peptide by restricting the flexibility and interfering with normal dynamic behavior by inhibiting the transition from the R-state to the T-state. In contrast, the application of oscillating field damages the peptide structure via the rapid re-alignment process that the peptide undergoes when responding to the instantaneous changes in electric field strength and direction. Both of these processes are dependent on the field strength. For the oscillating case, as the field gets stronger, the peptide undergoes faster re-alignment along the field direction with minimal lag time when the direction changes. In order to do so, the peptide has to readjust very rapidly following a pathway similar to that of a thermal stress response. In addition to the rapid alignment process, the peptide also experiences continuous stretching and relaxation of the helical region as the electric field oscillation reaches its peaks and zeros, which accelerates the unfolding process of the peptide. The study also highlighted the important role that helical residues play in the peptide interactions with the electric field.[5] The current work builds upon those results by investigating the effects of different frequencies of an electric field on peptide behavior. Specifically, we simulated the frequencies of 1.225 and 4.9 GHz (half and double the previously used frequency, respectively) and compared the results to those obtained at static and 2.45 GHz oscillating field conditions.[5]

2. Insulin

Insulin is an important hormone that regulates blood sugar and functions as a weak growth hormone. Its biological significance has led to numerous studies on the mechanism of insulin's formation and bioactivity.[4−9] The insulin monomer consists of two chains: chain-A with 21 amino acid residues and chain-B with 30 amino acid residues. They are connected by two interchain disulfide bonds between residues A7−B7 and residues A20−B19. In addition, one intrachain disulfide bond exists between residues A6−A11. It is believed that the active form of insulin is a monomer, based on studies of despentapeptide insulin, which lacks a dimer-forming region.[10] Due to insulin's solubility and propensity for self-association, obtaining crystal structures of an intact insulin monomer has proven difficult.[11] Thus, the structural knowledge of native insulin has been primarily inferred from NMR experiments on engineered monomeric insulin such as despentapeptide insulin.[12,13] In this study, we focus on the structure of insulin chain-B as there is experimental evidence that it is predominantly stable independently of chain-A.[7,14] Our previous study comparing the effect of chain-B isolation and thermal stress on insulin has also confirmed this property, although increased flexibility was

* Corresponding author. Telephone: +61 3 9925 2571. Fax: +61 3 9925 5290. E-mail: irene.yarovsky@rmit.edu.au.
[†] RMIT University.
[‡] Cytopia Research Pty. Ltd.

10.1021/jp067248g CCC: $37.00
Published on Web 05/02/2007

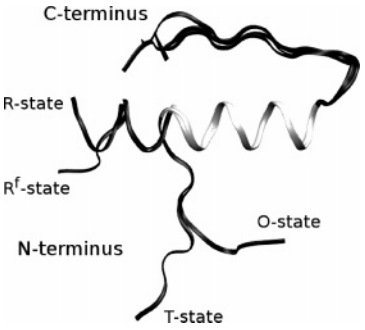

Figure 1. Commonly occurring conformations of insulin chain-B. The main conformations are the R- and the T-states. The central B9−B19 helix is highlighted in light gray.

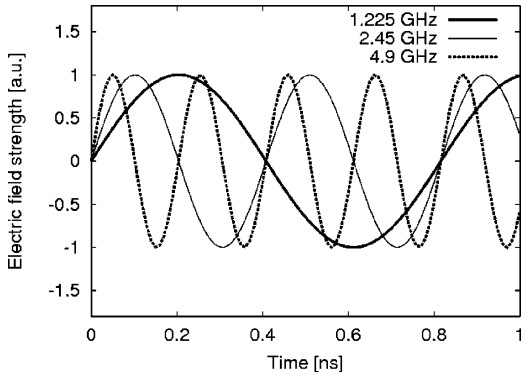

Figure 2. Comparison of oscillating field frequencies of 2.45, 1.225, and 4.9 GHz.

observed in the terminal regions.[15] There are many known conformations of chain-B, defined by the structure of the N-terminus. The main conformations are the R- and T-states.[16] In the R-state, residues B1−B8 are in a helical conformation, while in the T-state, these residues are in an extended conformation. The T-state is thought to be the active state, as it is believed to be the conformation adopted by monomeric insulin.[12] Experimentally derived structures of chain-B, shown in Figure 1, illustrate the range of conformations which occur in this peptide, including the starting structure used in the simulations. Our previous work has also indicated that a T-like state better satisfies the nuclear magnetic resonance (NMR) experimental data of bovine insulin chain-B in solution, compared to any other conformation.[4]

3. Methods

This study utilizes a classical molecular dynamics algorithm[17,18] as implemented in NAMD.[19] The well-validated, empirical, all-atom CHARMM27 forcefield[20] was chosen to represent the interactions between atoms. Between 10 Å and 12 Å, the nonbonded potential function was multiplied by a linearly decaying switching function, which results in no interaction beyond 12 Å. A neighbor list was maintained for atoms within 14 Å radius.

The SHAKE algorithm[21] was employed to restrain the lengths of bonds involving hydrogen atoms to their energy-minimized values. This allowed us to ignore the vibrational modes of hydrogen bonds and use a time step of 2 fs for all the simulations. Particle mesh Ewald summation was employed to account for long-range electrostatics.[22−24] The starting structure coordinates for each system were taken from the Protein Data Bank.[25] We have chosen the B-chain of wild boar insulin hormone (PDB code 1ZNI[26]) for our study. This particular insulin structure has an R^f-form,[6,8] with residues B1−B3 and B24−B30 in extended conformation, residues B4−B19 in α-helical conformation, and residues B20−B23 forming a turn (Figure 1).

TABLE 1: Details of Simulation Systems and Conditions

$f = 1.225$ GHz		$f = 4.9$ GHz		
system name	simulation length [ns]	system name	simulation length [ns]	electric field strength, E_{RMS} [V/m]
O2H	10	O2D	10	5×10^8
O3H	10	O3D	10	10^8
O4H	10	O4D	10	5×10^7
O5H	10	O5D	10	10^7

The peptide was enclosed in a periodic box sized 60 Å × 60 Å × 60 Å. After filling the box with 7002 TIP3P[27] water molecules (corresponding to water density of 1.0 g/cm^3), the whole system was energy minimized for 20000 steps by way of conjugate gradient and line search algorithms. Two equilibration stages were then performed successively, each lasting 600 ps at a temperature of 300 K. The first of these stages was performed in a constant volume (NVT) ensemble. This was then followed by a constant pressure (NPT) equilibration at 1 bar, utilizing the Nosé−Hoover method of pressure control, in which fluctuations in the barostat are controlled by Langevin dynamics.[28] The 10-ns dynamics (data collection) stage was then performed in a constant pressure (NPT) ensemble set to 1 bar with a Berendsen thermal bath coupling[29] to 300 K. The atomic coordinates were saved every 2500 steps (5 ps) for analysis, resulting in 2000 trajectory frames for each system. The methodology has been validated in our previous studies,[4,5] which reproduced the known flexibility of insulin, with the majority of the sampled conformations satisfying the nuclear Overhauser effect (NOE) distance restraints obtained by NMR spectroscopy,[7] and effectively simulated the effects of static and oscillating electric field stresses.

The labeling system follows the convention used in our previous work.[5] The oscillating field frequencies of 1.225 and 4.9 GHz correspond to periods of 816.32 and 204.08 ps, respectively. These are half and double the frequency of the electric field used in our previous study.[5] The original frequency of 2.45 GHz was used in previous experimental work investigating the effect of microwave radiations on various proteins.[30] As a comparison, digital mobile phones operate at frequencies ranging between 1.8 and 1.9 GHz with the third-generation systems using up to 2.2 GHz. The difference between the three electric field frequencies used in this study is illustrated in Figure 2. The details of the simulations performed are summarized in Table 1. In the system names, the letter "O" denotes oscillating electric field, the letter "H" denotes half of the original electric field frequency (i.e., a frequency of 1.225 GHz), and the letter "D" denotes double the original electric field frequency (i.e., frequency of 4.9 GHz). The electric field strengths shown are the root-mean-square (rms) values, obtained by the simple relation: $E_{RMS} = ((E_{max})/(\sqrt{2}))$. The numbers 2−5 denote the strength of the applied electric fields, ranging between 10^7 to 5×10^8 V/m, as shown in Table 1. These values of electric field strength were taken from our previous paper.[5] In addition to these systems, we will refer to the reference systems without applied electric field as N300 (for the system at 300 K) and N400 (for the system at 400 K), as used in our previous work.

4. Results and Discussion

4.1. Secondary Structure Analysis. Figure 3 shows the secondary structure evolution of the systems described in Table

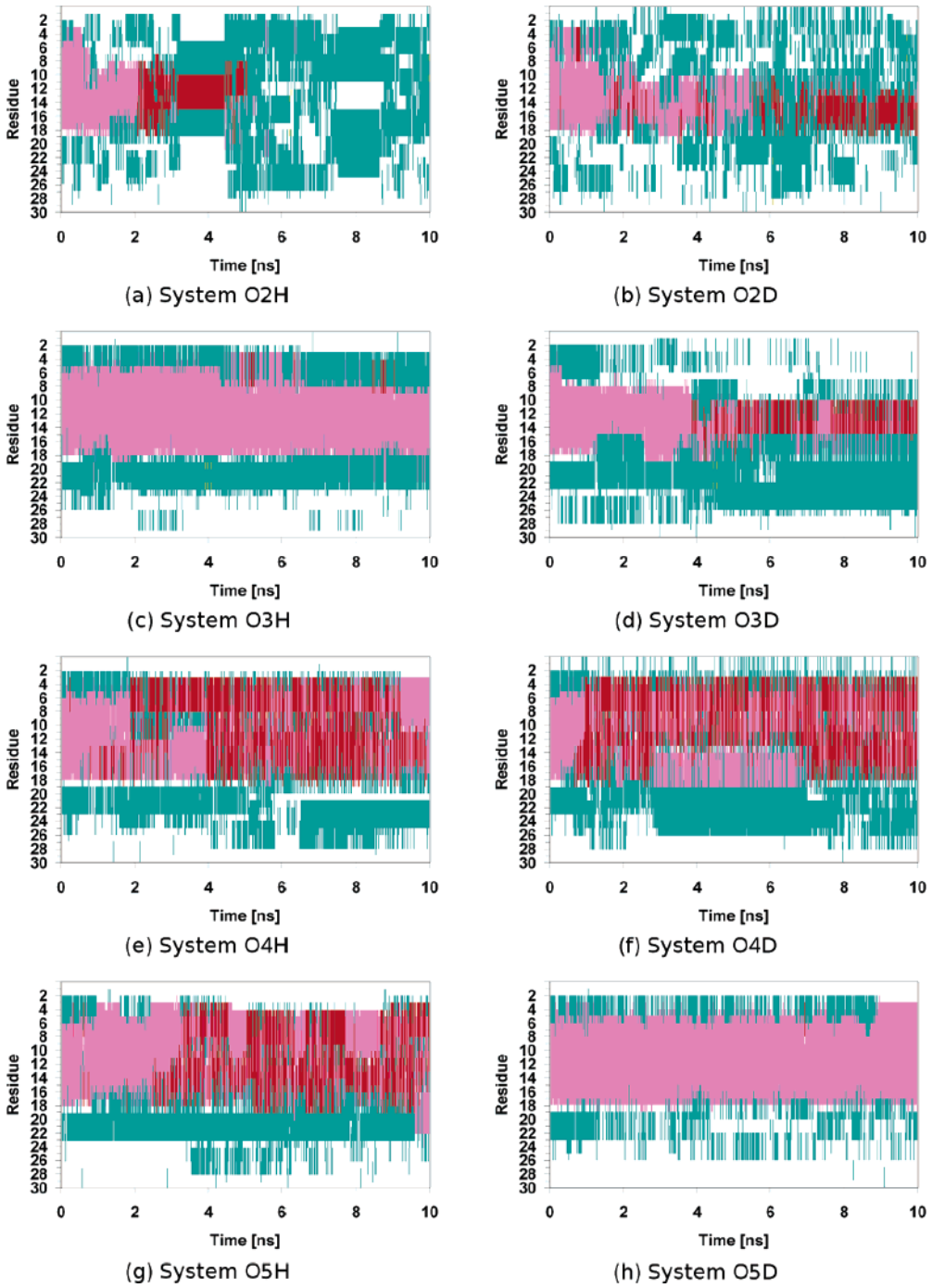

Figure 3. Evolution of secondary structure of insulin chain-B under oscillating field of frequencies 1.225 and 4.9 GHz. The colors denote the following secondary structures: magenta: α-helix, red: π-helix, cyan: turn, white: coil.

1. The secondary structure was classified by VMD[31] using the STRIDE algorithm which utilizes hydrogen-bond energy and main-chain dihedral angles in addition to hydrogen-bond distances.[32] In all of the systems presented we observed similarities with their evolution under an applied oscillating field of 2.45 GHz, described in our previous work.[5]

Specifically, under high electric field strength, systems O2H and O2D exhibited disruption to the secondary structure. In the system with an electric field frequency of 1.225 GHz, the helical region is lost within 5 ns (6.2 electric field oscillations). Interestingly, at 10^8 V/m, secondary structure disruption was only observed in system O3D with an electric field frequency of 4.9 GHz. This disruption was not observed in system O3H, where instead the α-helix is conserved, similar to the stabilizing effect of a static field.[5] The helix-breaking event at the glycine residue B8 is an important first step for the R-to-T transition, the active state of insulin characterized by the change in conformation of B1−B8 residues to extended structure.[10] In order for the transition from the R- or R^f-state to the T-state to occur, the helix pivots at Gly 8, and the residues B1−B8 become fully extended (see Figure 1). The break in the helix was previously observed in our simulations under ambient conditions[10] and also in the systems under the application of 2.45 GHz oscillating field of strength lower than 10^8 V/m.[5] The snapshots of insulin chain-B conformation of systems O2H, O2D, O3H, and O3D at 6 ns are shown in Figure 4.

The difference in behavior of insulin chain-B under an oscillating electric field of different frequencies is intrinsically

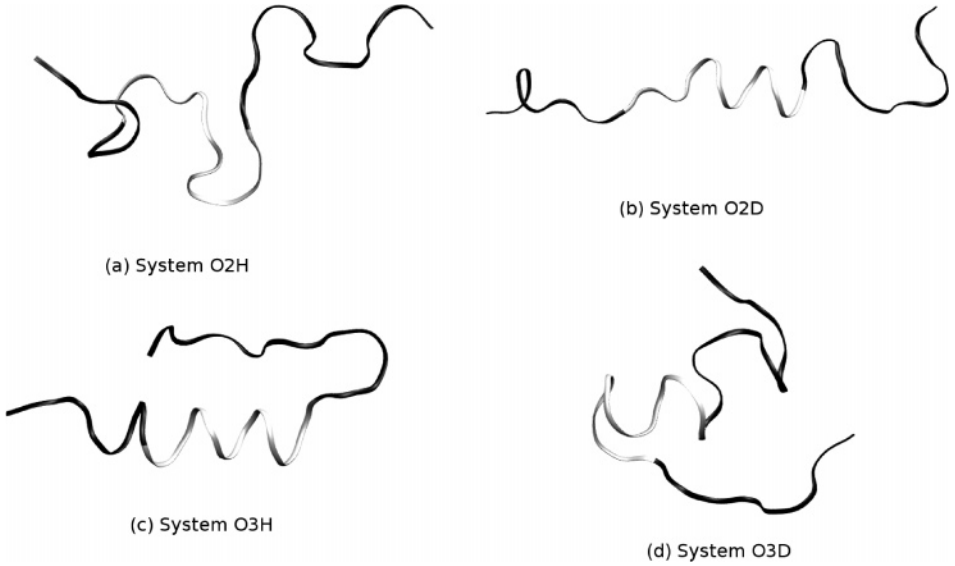

Figure 4. Snapshots of the insulin chain-B conformations at 6 ns for systems O2H, O2D, O3H, and O3D. Disruption to the secondary structure is observed in all systems except O3H. Residues B9−B19 are highlighted in light gray.

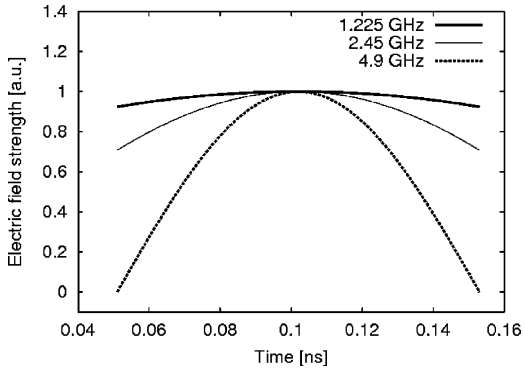

Figure 5. Comparison of the oscillating fields of different frequencies shows that within the same time period of 100 ps, the low-frequency oscillating field does not change as rapidly as the high-frequency oscillating field. The maximum of each electric field frequency has been aligned with respect to that of 4.9 GHz.

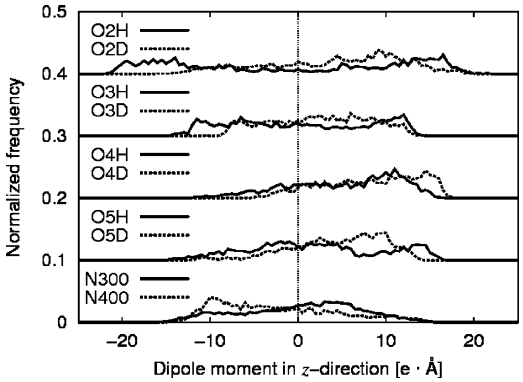

Figure 6. B9−B19 helical dipole moment distribution in the *z*-direction of insulin chain-B under oscillating electric field of frequencies 1.225 and 4.9 GHz. Each plot is displaced by 0.1 to improve clarity. Positive dipole moment signifies positive correlation with the electric field.

related to the nature of the field. Figure 5 illustrates that within the same time frame of approximately 100 ps, the instantaneous change in the strength of the low-frequency electric field does not happen as rapidly as does the strength of the high-frequency field. As a result, compared to the high-frequency electric field, the application of the low-frequency field within the time frame of 100 ps resembles a static electric field. Within the simulation time frame of 10 ns, the systems with the low-frequency electric field spend less time experiencing instantaneous changes in the strength of the electric field than do the systems under the high-frequency electric field. Consequently, the α-helical content is maintained, in a manner similar to that resulting from the stabilizing effect of the static field, thus restricting access to bioactive conformations.[5]

The application of oscillating field strength of lower than 10^8 V/m also showed no helix-breaking event, although the α- to π-helix transitions occurred in all systems except O5D. The α- to π-helix transition has been observed in experimental studies,[33,34] as well as in our previous work,[4,5] which indicates that it represents a genuine conformational feature rather than an artifact of a specific forcefield.[35]

4.2. Dipole Moment Distribution. Due to the helical nature of the central region of insulin chain-B, the peptide possesses a strong dipole moment which has a potential to be affected by electric fields. The dipole moment value distribution in the applied field direction can be used as a measure of the alignment of the peptide with respect to the field. Figure 6 shows such a distribution of dipole moment values of the B9−B19 helix in the direction of applied field (*z*-axis) for all the systems over the data collection stage. The dipole moment distributions have been normalized to allow direct comparison between different electric field strengths. The dipole moment distributions for the reference systems at 300 and 400 K from the previous work have been reproduced here for comparison.[5]

The distributions of the dipole moment show either a single broad peak or a double peak, which is characteristic of oscillating field systems. The double peaks were observed primarily in the systems with an electric field frequency of 1.225 GHz at relatively high field strengths, emphasizing the continuous realignment of the helix with respect to the field. The remaining systems show a skewed distribution, which results from the lag time of the peptide response as it aligns with respect to the applied electric field. Systems O2H and O3H exhibit stronger correlation with the applied field, compared to systems O2D and O3D. This is due to the longer time spent by the peptide under the influence of the field without the field's direction being changed.

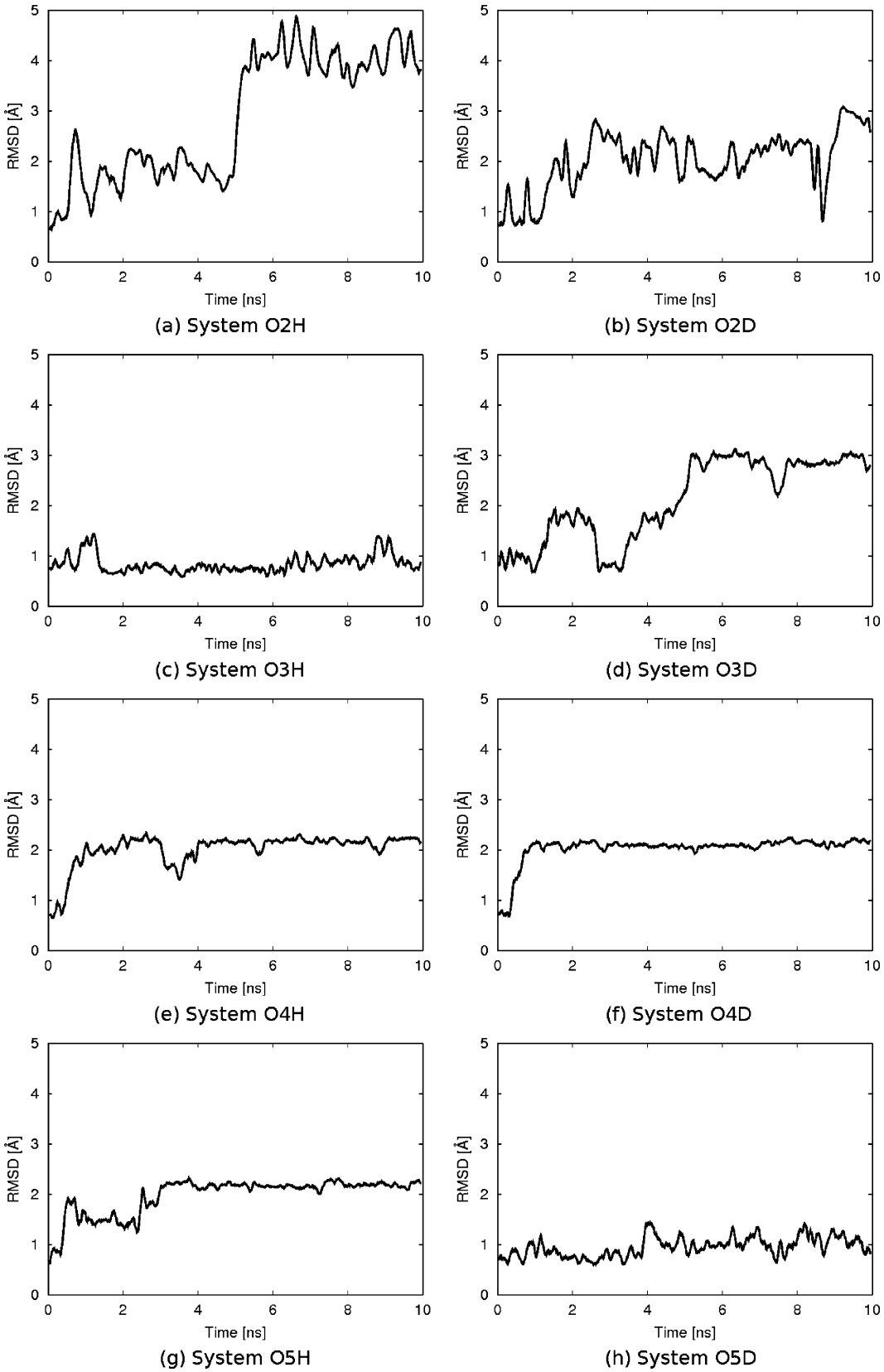

Figure 7. 100-ps running average of the B9−B19 helix backbone rmsd of the insulin chain-B systems under oscillating electric field of frequencies of 1.225 and 4.9 GHz.

4.3. Root-Mean-Square Deviation. The structural stability of the B9−B19 helical region was investigated by determining the root-mean-square deviation (rmsd) of the backbone atoms relative to that at the start of the data collection stage. The plots of the rmsd's as a function of time are presented in Figure 7. The rmsd's show variability that is comparable with that of the rmsd's of the systems under the oscillating field of 2.45 GHz presented in our previous article[5] which can be expected due to the oscillatory nature of the electric field. Most systems showed relative stability in the rmsd values by the end of the

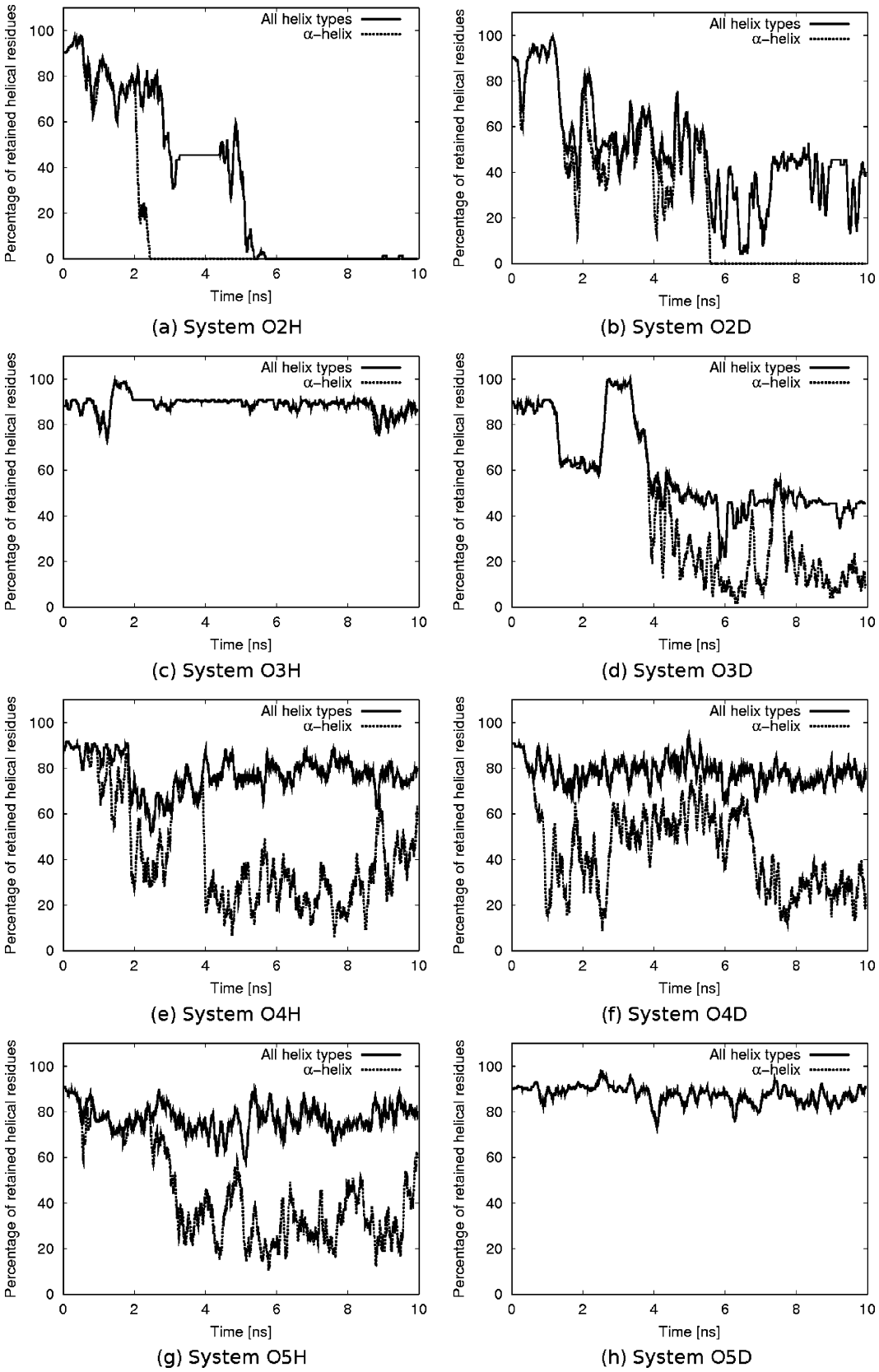

Figure 8. 100-ps running average of the B9−B19 helical content retained as a function of time for the insulin chain-B systems under oscillating electric field of frequencies 1.225 and 4.9 GHz. Black lines indicate the all-helical content, and the dotted lines indicate the α-helical content.

simulation time frame, especially the systems with moderately low electric field strengths. In system O2H, a jump in rmsd value at 5 ns was observed, corresponding to the disruption of the helical region. A smaller jump observed in system O3D is also related to changes in the secondary structure. Both of these conformations are shown in Figure 4.

The average rmsd values for the last nanosecond of the simulations are presented in Table 2. For comparison, the results

TABLE 2: B9−B19 Helix Backbone rmsd of the Insulin Chain-B Systems under Oscillating Electric Field of Various Frequencies, Averaged over the Last Nanosecond

	rmsd [Å]		
system name	_H (1.225 GHz)	_ (2.45 GHz)[a]	_D (4.9 GHz)
O2_	4.24 ± 0.35	4.33 ± 0.35	2.8 ± 0.2
O3_	0.9 ± 0.2	2.2 ± 0.1	2.93 ± 0.15
O4_	2.21 ± 0.09	1.41 ± 0.15	2.16 ± 0.09
O5_	2.2 ± 0.1	1.9 ± 0.4	1.0 ± 0.2
N300[a]		2.25 ± 0.08	
N400[a]		1.5 ± 0.6	

[a] Values reproduced from previous work.[5]

TABLE 3: Radius of Gyration of Insulin Chain-B, Averaged over Data Collection Stage, after the First Nanosecond

	r_g [Å]		
system name	_H (1.225 GHz)	_ (2.45 GHz)[a]	_D (4.9 GHz)
O2_	12.2 ± 1.7	13.8 ± 1.7	12.3 ± 2.0
O3_	10.5 ± 0.4	10.9 ± 0.8	10.5 ± 1.0
O4_	10.1 ± 0.4	9.9 ± 0.5	10.3 ± 0.4
O5_	10.6 ± 0.7	10 ± 1	9.94 ± 0.35
N300[a]		9.7 ± 0.5	
N400[a]		11.0 ± 1.3	

[a] Values reproduced from previous work.[5]

from our previous work have also been reproduced in the table.[5] The complete loss of helical residues in system O2H is reflected in the high rmsd that is similar to that obtained for system O2. This high rmsd value was caused by the constant realignment of insulin chain-B with respect to the applied electric field. In contrast, system O2D retained some helical content, and the rmsd was not as high as in systems O2 and O2H. At 10^8 V/m, the application of higher-frequency electric field (system O3D) caused more disruption to the secondary structure compared to the disruption in systems O3H and O3. In contrast, system O3H showed helix conservation, similar to that of the corresponding static field system,[5] resulting in an rmsd that was lower than that of the other systems.

4.4. Radius of Gyration. Table 3 presents the average r_g of each isolated chain-B system under oscillating electric field after the first nanosecond, along with the corresponding values of the reference systems for comparison. The r_g of the systems under oscillating field frequencies of 1.225 and 4.9 GHz are almost identical and agree quite well with the r_g for systems under the field frequency of 2.45 GHz. They all showed a larger r_g compared to that of system N300, although within the limits set by the variance. The systems also showed a lower threshold of conformational disruption than did the static field systems.[5] It is interesting to note that system O3D showed a value of r_g comparable to that of the N300 system, even though the rmsd value of the B9−B19 backbone indicated relatively large disruption. This can be explained by insulin chain-B adopting a compact conformation where the terminal regions are folded toward the main helix, as illustrated in Figure 4.

4.5. Helical Content. The STRIDE algorithm[32] was employed to obtain the number of retained helical residues of each insulin chain-B system under the application of the oscillating field as a measure of the stability of the helix over the data collection stage. The retained numbers of all-helical (consisting of α-, π-, and 3_{10}-helices) and α-helical residues of insulin chain-B over the data collection stage are presented in Table 4, along with the values for the reference systems.

The retained numbers of all-helical residues exhibit values and trends similar to those obtained from the simulations with the oscillating field frequency of 2.45 GHz. However, there is more variation in the retained number of α-helical residues in the systems under oscillating field frequencies of 1.225 and 4.9 GHz, compared to the systems under the 2.45 GHz field frequency. This is a reflection of the high degree of α- to π-helix transition observed in these systems.

At field strength of 10^8 V/m, significant variations were observed at different frequencies. At a low frequency of 1.225 GHz (system O3H), a stable α-helix was observed which was preserved until the end of the simulation. This helix stability is nearly as prominent as it is in the case of a static field, whereby system O3H preserved an average of 11.6 α-helical residues compared to 12.7 residues preserved by the application of static electric field of the same effective strength.[5] At a field frequency of 2.45 GHz, 8.0 α-helical residues were maintained. At a higher frequency of 4.9 GHz, only an average of 4.9 α-helical residues was retained. This illustrates that at a field strength of 10^8 V/m, increasing the frequency of the electric field leads to increasing the distortion of the secondary structure of isolated insulin chain-B. At the same time, the lower frequency has a stabilizing effect similar to that of the static field, which may restrict normal peptide behavior.

In order to understand the details of the changes to the central B9−B19 helix, the plots of all-helical and α-helical residues of each system as a function of time are presented in Figure 8.

The all-helical residues are maintained at 80% (8.8 residues) throughout the simulation in all systems except for O2H, O2D, and O3D, where a significant disruption to the secondary structure was observed, similar to that of the systems at 2.45 GHz. The α-helical content is generally reduced to 30% (3.3 residues) by the end of the simulation, due to the presence of α- to π-helix transition. However, in systems O3H and O5D, the α-helical content was retained until the end of the simulation.

Figure 9 shows the retained hydrogen bonds between the backbone atoms of residues B9−B19 for systems O2H, O2D, O3H, and O3D. The plots demonstrate correlation between the

TABLE 4: Retained Number of All-Helical and α-Helical Residues for Insulin Chain-B under Oscillating Field of Various Frequencies, Averaged over the Data Collection Range

	retained all-helical residues			retained α-helical residues		
system name	_H (1.225 GHz)	_ (2.45 GHz)[a]	_D (4.9 GHz)	_H (1.225 GHz)	_ (2.45 GHz)[a]	_D (4.9 GHz)
O2_	4.0 ± 4.5	3.9 ± 4.2	5.9 ± 3.7	2.2 ± 4.3	3.5 ± 4.3	3.9 ± 4.6
O3_	11.8 ± 2.0	11.8 ± 2.2	6.7 ± 2.6	11.6 ± 2.0	8.0 ± 4.3	4.9 ± 4.3
O4_	12.6 ± 1.9	12.8 ± 2.3	12.7 ± 2.1	6.7 ± 4.7	12.7 ± 2.4	6.6 ± 4.4
O5_	12.4 ± 2.0	9.5 ± 1.9	12.8 ± 1.3	7.4 ± 4.8	9.4 ± 1.8	12.7 ± 1.3
N300[a]		11.4 ± 2.7			8.3 ± 3.9	
N400[a]		8.8 ± 2.4			7.9 ± 2.7	

[a] Values reproduced from previous work.[5]

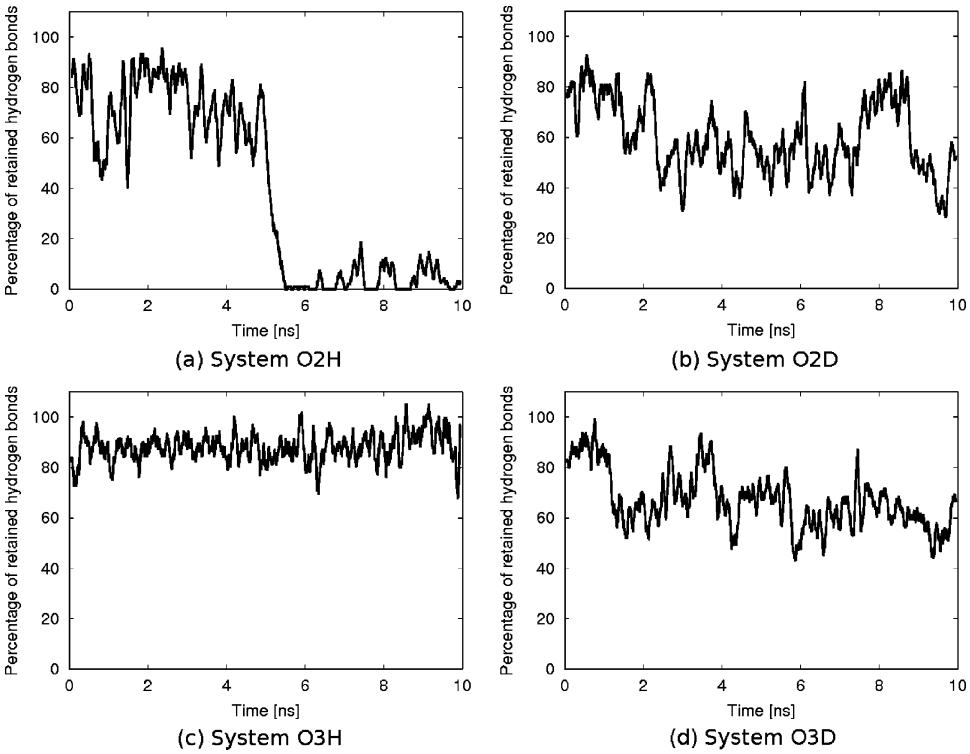

Figure 9. 100-ps running average of the retained B9−B19 helical backbone hydrogen bonds as a function of time for insulin chain-B systems under electric field of frequencies 1.225 and 4.9 GHz with strength equal to or above 10^8 V/m.

TABLE 5: Percentage of Solvent Accessible Surface Area Throughout the Data Collection Stage after the First Nanosecond, Relative to That in the N300 Simulation

	percentage SASA (relative to N300)		
system name	_H (1.225 GHz)	_ (2.45 GHz)[a]	_D (4.9 GHz)
O2_	116.9 ± 8.8	120.9 ± 8.3	114.8 ± 6.6
O3_	104.9 ± 3.1	107.7 ± 6.1	108.1 ± 9.2
O4_	101.9 ± 6.0	100.7 ± 4.4	97.5 ± 2.5
O5_	107.2 ± 3.6	105.1 ± 6.4	100.3 ± 4.3
N300[a]		100.0 ± 5.8	
N400[a]		107.7 ± 6.6	

[a] Values reproduced from previous work.[5]

loss of hydrogen bonds between the backbone atoms with the disruption of the helical region.

4.6. Solvent-Accessible Surface Area (SASA). The SASA was calculated using the program X-PLOR[36] for the data collection stage after the first nanosecond. For clarity, the resulting SASA and variance are expressed as a percentage of the SASA of the N300 system (see Budi et al.[5]) and are presented in Table 5 along with the reference systems for comparison.

The new data presented in Table 5 correlate with the results obtained for the systems with applied oscillating field of frequency 2.45 GHz, with the exception of the system at 10^8 V/m. As already noted, at this strength the extent of changes sustained by insulin chain-B can be related to the frequency of the applied field. At the lowest frequency (1.225 GHz, system O3H), the SASA was minimally affected, with only a 4.9% increase relative to the SASA of the N300 system. At a field frequency of 2.45 GHz (system O3), the SASA increased by 7.7%. At the highest frequency of 4.9 GHz (system O3D), the increase in SASA is 8.1% relative to the SASA of the N300 system. It is also notable that, as the frequency increased, the variance in SASA also increased.

5. Conclusion

In this work, we have expanded on our previous study (investigating the effects of electric field stress on proteins) by examining the effects on insulin chain-B of oscillating electric field frequencies of 1.225 and 4.9 GHz. The behavior at low field strengths at these frequencies is similar to that under an oscillating electric field of a frequency of 2.45 GHz, suggesting that the oscillatory nature of the electric field has a more destabilizing effect on the peptide than do static fields of the same effective strength.

At high field strengths, stronger interactions of the helical region of the peptide were observed with the applied field of frequency 1.225 GHz than with the field of frequency 4.9 GHz, in terms of the peptide alignment with respect to the field direction and restriction of mobility. This is believed to be because at a lower frequency, the peptide is exposed to less instantaneous changes to the strength of the electric field. This is particularly relevant as the oscillation reaches its maximum. Consequently, some of the systems exhibited a restriction to the peptide mobility similar to that observed in the static field simulations, inhibiting transition to the bioactive conformation. In contrast, at high frequency, the peptide is exposed to more instantaneous changes to the strength of electric field. In this case, the field changes direction rapidly and accelerates the destabilization of the peptide structure.

Acknowledgment. We thank Dr. Andrew Hung and Ms. Nevena Todorova of RMIT University for their useful feedback and discussions. We also acknowledge the Australian Research Council and Cytopia Research Pty. Ltd., for providing financial support for this project, and the Australian Partnership for Advanced Computing for the generous grant of computer time.

References and Notes

(1) de Pomerai, D. I.; Smith, B.; Dawe, A.; North, K.; Smith, T.; Archer, D. B.; Duce, I. R.; Jones, D.; Candido, E. P. *FEBS Lett.* **2003**, *543*, 93.

(2) Salford, L. G.; Brun, A. E.; Eberhardt, J. L.; Malmgren, L.; Persson, B. R. R. *Environ. Health Perspect.* **2003**, *111*, 881.

(3) Laurence, J. A.; French, P. W.; Lindner, R. A.; McKenzie, D. R. *J. Theor. Biol.* **2000**, *206*, 291.

(4) Legge, F. S.; Budi, A.; Treutlein, H.; Yarovsky, I. *Biophys. Chem.* **2006**, *119*, 146.

(5) Budi, A.; Legge, F. S.; Treutlein, H.; Yarovsky, I. *J. Phys. Chem. B* **2005**, *109*, 22641.

(6) Ciszak, E.; Beals, J. M.; Frank, B. H.; Baker, J. C.; Carter, N. D.; Smith, G. D. *Structure* **1995**, *3*, 615.

(7) Hawkins, B.; Cross, K.; Craik, D. *Int. J. Pept. Protein Res.* **1995**, *46*, 424.

(8) Whittingham, J. L.; Chaudhuri, S.; Dodson, E. J.; Moody, P. C. E.; Dodson, G. G. *Biochemistry* **1995**, *34*, 15553.

(9) Derewenda, U.; Derewenda, Z.; Dodson, E. J.; Dodson, G. G.; Reynolds, C. D.; Smith, G. D.; Sparks, C.; Swenson, D. *Nature* **1989**, *338*, 594.

(10) Jørgensen, A. M. M.; Olsen, H. B.; Balschmidt, P.; Led, J. J. *J. Mol. Biol.* **1996**, *257*, 684.

(11) Olsen, H. B.; Ludvigsen, S.; Kaarsholm, N. C. *Biochemistry* **1996**, *35*, 8836.

(12) Hua, Q. X.; Weiss, M. A. *Biochemistry* **1991**, *30*, 5505.

(13) Hua, Q.-X.; Hu, S.-Q.; Frank, B. H.; Jia, W. H.; Chu, Y.-C.; Wang, S.-H.; Burke, G. T.; Katsoyannis, P. G.; Weiss, M. A. *J. Mol. Biol.* **1996**, *264*, 390.

(14) Qiao, Z.-S.; Min, C.-Y.; Hua, Q.-X.; Weiss, M. A.; Feng, Y.-M. *J. Biol. Chem.* **2003**, *278*, 17800.

(15) Budi, A.; Legge, S.; Treutlein, H.; Yarovsky, I. *Eur. Biophys. J. Biophys. Lett.* **2004**, *33*, 121.

(16) Kaarsholm, N. C.; Ko, H.-C.; Dunn, M. F. *Biochemistry* **1989**, *28*, 4427.

(17) Allen, M. P.; Tildesley, D. J. *Computer Simulation of Liquids*; Oxford University Press: New York, 1989.

(18) Leach, A. R. *Molecular Modelling: Principles and Applications*, 2nd ed.; Prentice Hall: Harlow, England, 2001.

(19) Kalé, L.; Skeel, R.; Bhandarkar, M.; Brunner, R.; Gursoy, A.; Krawetz, N.; Phillips, J.; Shinozaki, A.; Varadarajan, K.; Schulten, K. *J. Comput. Phys.* **1999**, *151*, 283.

(20) MacKerell, A. D., Jr.; Bashford, D.; Bellott, M.; Dunbrack, R. L., Jr.; Evanseck, J. D.; Field, M. J.; Fischer, S.; Gao, J.; Guo, H.; Ha, S.; Joseph-McCarthy, D.; Kuchnir, L.; Kuczera, K.; Lau, F. T. K.; Mattos, C.; Michnick, S.; Ngo, T.; Nguyen, D. T.; Prodhom, B.; Reiher, W. E., III; Roux, B.; Schlenkrich, M.; Smith, J. C.; Stote, R.; Straub, J.; Watanabe, M.; Wiórkiewicz-Kuczera, J.; Yin, D.; Karplus, M. *J. Phys. Chem. B* **1998**, *102*, 3586.

(21) Ryckaert, J.-P.; Ciccotti, G.; Berendsen, H. J. C. *J. Comput. Phys.* **1977**, *23*, 327.

(22) Darden, T.; York, D.; Pedersen, L. *J. Chem. Phys.* **1993**, *98*, 10089.

(23) Essmann, U.; Perera, L.; Berkowitz, M. L.; Darden, T.; Lee, H.; Pedersen, L. G. *J. Chem. Phys.* **1995**, *103*, 8577.

(24) Petersen, H. G. *J. Chem. Phys.* **1995**, *103*, 3668.

(25) Berman, H. M.; Westbrook, J.; Feng, Z.; Gilliland, G.; Bhat, T. N.; Weissig, H.; Shindyalov, I. N.; Bourne, P. E. *Nucleic Acids Res.* **2000**, *28*, 235.

(26) Bentley, G.; Dodson, E.; Dodson, G.; Hodgkin, D.; Mercola, D. *Nature* **1976**, *261*, 166.

(27) Jorgensen, W. L.; Chandrasekhar, J.; Madura, J. D.; Impey, R. W.; Klein, M. L. *J. Chem. Phys.* **1983**, *79*, 926.

(28) Feller, S. E.; Zhang, Y. H.; Pastor, R. W.; Brooks, B. R. *J. Chem. Phys.* **1995**, *103*, 4613.

(29) Berendsen, H. J. C.; Postma, J. P. M.; Vangunsteren, W. F.; DiNola, A.; Haak, J. R. *J. Chem. Phys.* **1984**, *81*, 3684.

(30) Berry, Y. C. Personal communication.

(31) Humphrey, W.; Dalke, A.; Schulten, K. *J. Mol. Graphics* **1996**, *14*, 33.

(32) Frishman, D.; Argos, P. *Proteins: Struct., Funct., Genet.* **1995**, *23*, 566.

(33) Fodje, M. N.; Al-Karadaghi, S. *Protein Eng.* **2002**, *15*, 353.

(34) Armen, R.; Alonso, D. O. V.; Daggett, V. *Protein Sci.* **2003**, *12*, 1145.

(35) Feig, M.; MacKerell, A. D., Jr.; Brooks, C. L. *J. Phys. Chem. B* **2003**, *107*, 2831.

(36) Brünger, A. T. *X-PLOR*, Version 3.1: A system for X-ray crystallography and NMR; Yale University Press: New Haven, CT, 1992.